

Muscles in Action

Mia Chiquier
Columbia University

mia.chiquier@cs.columbia.edu

Carl Vondrick
Columbia University

vondrick@cs.columbia.edu

Abstract

Small differences in a person’s motion can engage drastically different muscles. While most visual representations of human activity are trained from video, people learn from multimodal experiences, including from the proprioception of their own muscles. We present a new visual perception task and dataset to model muscle activation in human activities from monocular video. Our Muscles in Action (MIA) dataset consists of 2 hours of synchronized video and surface electromyography (sEMG) data of subjects performing various exercises. Using this dataset, we learn visual representations that are predictive of muscle activation from monocular video. We present several models, including a transformer model, and measure their ability to generalize to new exercises and subjects. Putting muscles into computer vision systems will enable richer models of virtual humans, with applications in sports, fitness, and AR/VR.

1. Introduction

Human motion is created by and constrained by muscles. People’s understanding of human motion is equal parts observation and sensation. The vision community has made great progress in modelling and analyzing human motion from video via tasks such as pose estimation, action recognition and more. However, human understanding of motion goes beyond the surface – we are able to predict how other humans physically feel just by observing them. Every action activates our muscles, and if we want to learn truly accurate representations of human motion, then we need to model human body internals as well. In this work, we learn to predict the muscle activation of human motion from video.

Better understanding human muscle activity from vision can enable many new exciting applications. Most immediately, in sports and dance, specific minor differences in pose can yield drastic differences in muscle activation and result in incorrect exercises and injuries, yet other minor differences in pose do not interfere with the correctness of the exercise. Correctly predicting muscle activation from video

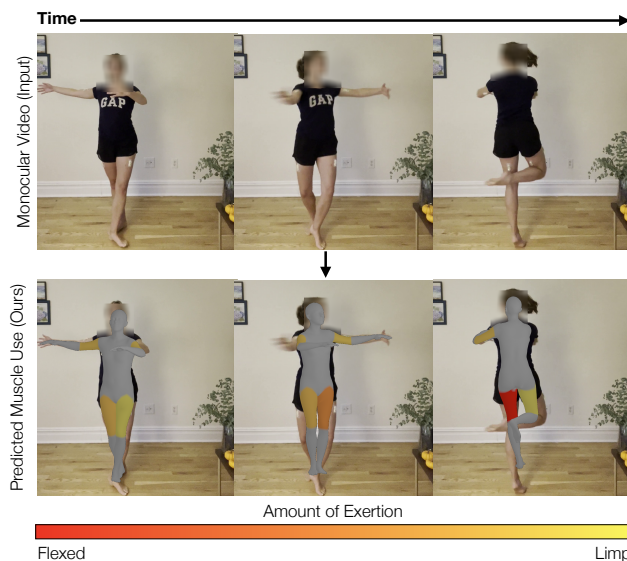


Figure 1. **Muscles in Action:** From just a glance at a video of a person performing an activity, we can often have intuitions about whether a person is flexing a muscle, or whether a muscle is limp. In this paper, we introduce a model and dataset for inferring muscle exertion. The bottom row shows the predicted output from our system. Modeling the relationship between the visual and muscle modality can be useful many applications, such as assistive technology, or disentangling the forces underlying human motion.

would enable the development of machine perception systems capable of recommending exercises that target or avoid particular muscle groups, as well as provide critical pose correction. Furthermore, leveraging muscle activity prediction in representations of human motion could be useful for downstream tasks such as imitation learning and modelling virtual humans for AR/VR applications.

The standard way of measuring muscle activity is through the use of electromyography sensors. They exist in both invasive form and non-invasive form called surface electromyography, sEMG for short. While athletes do use these sensors occasionally to correct their own postures, they are cumbersome and expensive to acquire and wear. As such, we propose to predict sEMG signals from vision.

We collected a 2-hour dataset of synchronized single-view video and sEMG signals of 8 muscles of subjects performing various physical activities. The 8 muscles include the left and right biceps, the left and right triceps, the left and right quadriceps, and the left and right hamstrings, denoted in Figure 2. This dataset includes 20 different exercises, each performed by 2 subjects, as seen in Figure 3. We asked the subjects to vary in their execution of the performance (i.e. different speeds, different locations within the camera frame, variation in direction etc.).

We constructed several baseline models, including a Transformer, trained to regress the eight sEMG values over time, given a video of human motion. We evaluate our model separately on each exercise and report the root mean squared error per activity in Table 1. Next, we investigate our model’s capabilities by testing its performance on new exercises and subject. We demonstrate that our learning-based methods are able to generalize to out-of-distribution exercises via the leave-one-out method, also reported in Table 1. In addition, we study the ability of our model to transfer across new subjects. In this setting, we fine-tune a model trained on the first subject with data from a second subject and demonstrate that our method performs better than trained from scratch on just the second subject’s data. Finally, we analyze the similarities and differences between visual representations that are trained with and without muscle activation signals.

2. Related Work

Human Motion Prediction from Video. The field of computer vision has seen tremendous progress in inferring information about human motion from monocular video. One of the tasks is to regress human pose from video by regressing skeleton key-points and meshes [7, 7, 18, 21, 28, 35, 51]. A related task is action segmentation [24]. Other tasks that span from the pose estimation results include human motion transfer [1, 8, 26, 47] and even pose correction to make a given pose anatomically-correct [16, 37]. Additionally, action classification and recognition are examples of the vision community leveraging video to predict information about various human motions and behaviors [22, 23, 36, 44, 48], as well as action intentionality [10]. Others have even tried to predict the future actions in videos [3, 14, 20, 38, 46]. Closely related, Park et al. predict the 3D gravity direction from a moving first-person view using inverse dynamics [34].

Multi-Modal Representations. Multi-modal learning with video is a long-standing problem in computer vision. Some works predict other modalities from video, such as sound [11, 32] by using the natural temporal correspondence between video and sound, as well as video captioning [49]. Beyond prediction, multi-modal learning has been shown to improve video representations, for example from sound

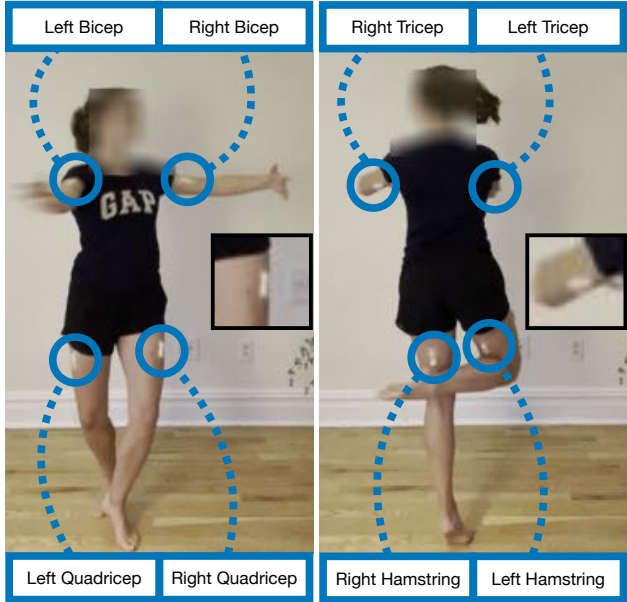


Figure 2. **Sensor Placement.** We illustrate the placement of our 8 sEMG sensors on a subject. We label the 8 measured muscles.

[5, 33], and language [42, 49]. The converse has also been explored - leveraging large datasets of unlabelled video has improved representations of other modalities [5, 6, 12, 29]. We are interested in predicting an entirely different modality from monocular video, muscle activation. In our analysis, we show this multi-modal signal can help visual representations better distinguish fine-grained activities.

Electromyography. To measure muscle activation, we use Surface Electromyography (sEMG) sensors, which are attached to electrodes placed on human skin to measure the electrical activity of muscle tissue. It is a very popular sensor for the opposite direction of the task in this paper: predicting pose from sEMG data [2, 4, 9, 27].

We are interested in the inverse direction - predicting sEMG from video. Previous work has considered this question, however, the input modality is not video. Some works use torque and/or surface force measurements as input [25, 40, 41], while others use goniometers to track pose [43] or motion capture tracking systems [17, 30, 50]. Our work seeks to predict muscle activation with no additional hardware at testing-time besides video.

Additionally, other works try to infer the weight of the object being lifted by a human from videos of muscles [2, 16], or predict muscle activation directly from 3D point clouds collected by depth cameras [31, 39]. However, these works rely on seeing the skin deformation on the human subject to infer muscle activity. We infer muscle activity from motion priors, not the visible increase in muscle size. This allows the algorithm to work for clothed humans, or humans performing physical activity at a distance.

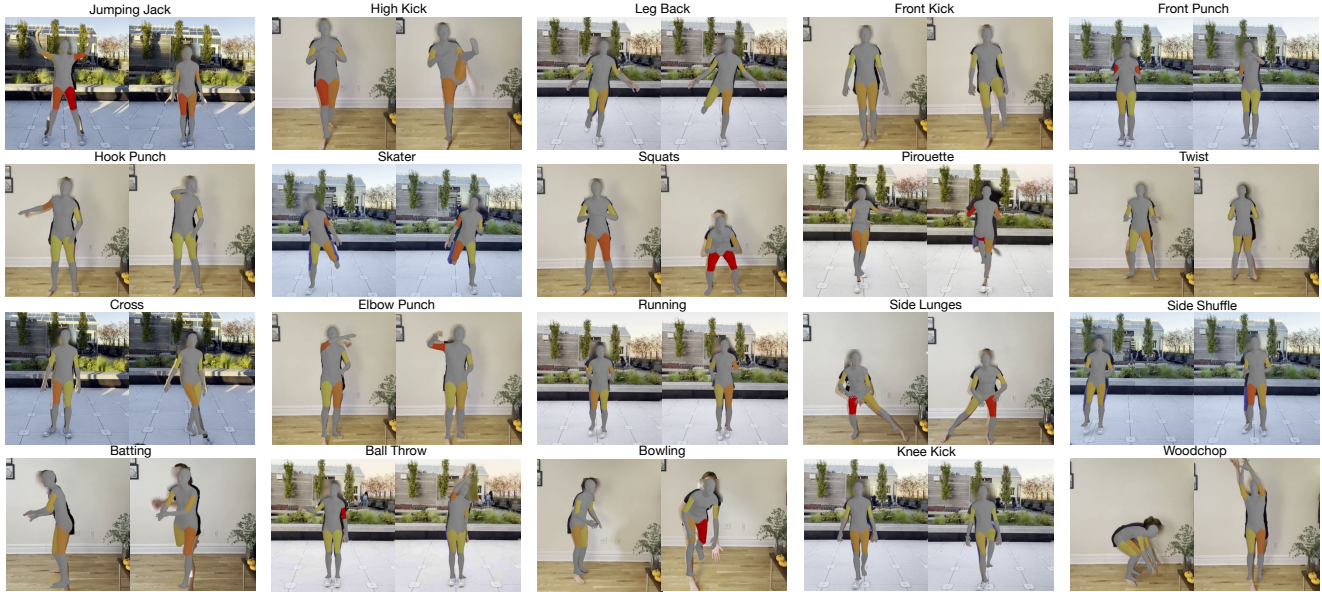


Figure 3. **The MIA Dataset.** We illustrate example exercises from our dataset for each of the 20 exercises.

3. The Muscles in Action (MIA) Dataset

In order to incorporate muscular information into representations of human motion, we need to obtain muscle activation signals that correspond to motion. As such, we collected a dataset of synchronized video and sEMG signals, which we open-source.

3.1. Data Collection

Our dataset consists of 2-hours of synchronized video and sEMG signals, for 8 muscles. These 8 muscles include both biceps, both triceps, both quads, and both hamstrings. The collected sEMG values correspond to the neuromuscular junction’s total bioelectric energy. The dataset is comprised of the following 20 exercises: jumping jack, high kick, leg back, front kick, front punch, hook punch, pirouette, skater, twist, squats, feet cross, elbow punch, side shuffle, batting, side lunge, running, ball throw, bowling, knee kick and woodchop. Please see Figure 5 for a canonical frame for each action.

Two subjects were involved in data collection. We collected 100 minutes of data for the first subject, and 20 minutes of data for the second subject. The first subject performed activity indoors, and the second subject performed activity outdoors. The subjects varied in body weight and muscle. The sensors were placed on the specified muscles, and not moved during the entire data collection process. We did our best to position the sensors in the same location on the muscle across both subjects.

To collect the EMG data, we used eight M40 Muscle Sense bluetooth wireless EMG sensors from AMR Corp. To collect the video, we used a standard iPhone 10 camera.

3.2. Data Preprocessing

We extract OpenPose [7] 2D keypoints by running VIBE’s [21] model on the videos. We normalize the raw sEMG data. For all experiments unless explicitly stated otherwise, the input sequence length is 30 frames and the output sequence length is 30 sEMG values per muscle, corresponding to 3 seconds.

4. Method

We present an approach for predicting muscle activity from videos. Let x_1, \dots, x_t be a sequence of images from a video of length t , and y_1^n, \dots, y_t^n be a sequence of sEMG data for muscle n . Our goal is to predict muscle activation y from x . The association between vision and muscle activity is rich and non-trivial. In order to solve this problem, our model needs to learn the relationship between patterns of motion and muscle activation. Some motion patterns, for example, active motion, will cause the muscles to be used. Other motions, such as dropping due to gravity, will still create motion but there will be little to no muscle activity. Motions occur from a variety of forces, and the model needs to distinguish whether the motion is caused by a person or by the world.

4.1. From Motion to Muscles

Similar motion patterns do not always yield similar muscle activations. For instance, while in two exercises a knee may be bent, this may not produce a quad activation in both cases for the bent leg. This divergence is illustrated in the first example in Figure 4, comparing the skater and

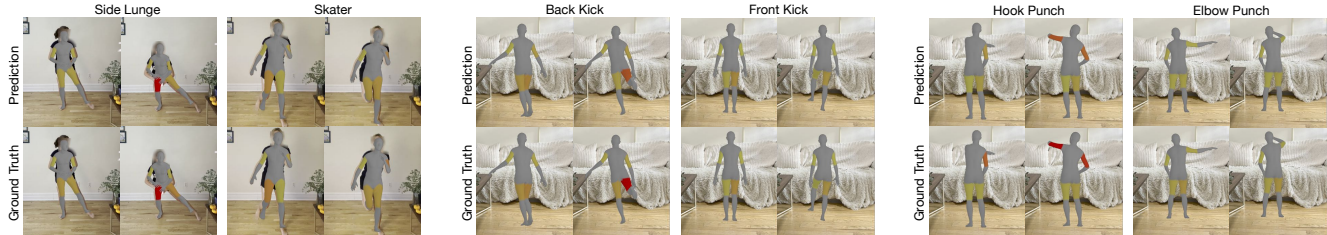


Figure 4. **Complex Motion to Muscle Mappings:** While two exercises can look similar, they can have very different muscle activations. On the left, we compare a side lunge and a skater, which both have a bent left leg in the frontal direction, but the left quad is only activated in the side lunge. In the middle, we compare a back kick and a front kick, which is the same motion except in opposite directions, yet the hamstring is only activated in the back kick. On the right, we compare a hook punch and an elbow punch, which are also the same motion except in opposite directions, yet the tricep is only active in the hook punch. These examples serve to illustrate a few of the complexities of the motion to muscle group activation mapping.

side lunge exercises. Small differences in relative foot positioning for similar motion patterns causes drastically different muscle activations. Additionally, for two almost identical motion paths, the direction of motion is crucial for determining whether a muscle group is active. For example, while a back kick will activate hamstrings, a front kick will not, as demonstrated in the second example in Figure 4. Moreover, for two almost identical motion patterns with the same direction, but with small differences in speed over time, also yields different muscle activations. An elbow punch pauses when the elbow is parallel to the shoulders, and does not activate the tricep, while a hook punch pauses when the elbow is in front of the chest, and does activate the tricep.

These nuances in very similar motion patterns create completely different muscle activation patterns, illustrating the richness of the task. Our model needs to differentiate across changes in space and time - it is not sufficient to understand that a limb is moving.

4.2. Architectural Desiratum

Our model needs to use the full temporal context, as muscle activation at time t does not just depend on the motion as time t , it also requires a knowledge of the motion p time bins in the past. This is because not only is past motion information important for identifying what muscle groups are currently engaged, but it is also crucial for understanding whether the current pose has been held for a while or not. Oftentimes, the muscle activity for a pose is highest at the onset of a new pose, decreases over time, and eventually begins to increase again as the pose becomes difficult to maintain.

Our model also needs to pay attention to spatial nuances, as previously demonstrated with the skater and side lunge comparison. Specifically in that example, we showed that relative positioning of feet conveys information about which leg is the supporting one, which is crucial to understanding whether a bent leg is contracting to push back

against gravity. However, these spatial features are not limb-invariant. While a difference in the vertical position of feet makes a difference for force understanding, a difference in vertical positioning of hands will not interplay with gravity in the same way for standing aerobics. As such, our model must not be spatially invariant.

4.3. Architecture

Our architecture is factored into two parts, a local motion encoder, and a global feature encoder. Our prediction for muscle activity is given by:

$$\hat{y} = f_{\psi}(g_{\theta}(x)) \quad (1)$$

where g_{θ} is our local motion encoder, and f_{ψ} is our global feature network. See Figure 5 for an overview of our architecture.

The local motion encoder is composed of a pretrained 2D keypoint extractor network, denoted by v , using the open-sourced VIBE checkpoints [21], followed by a temporal convolutional layer. The keypoints computed from $v(x)$ are a matrix of size $\mathbb{R}^{k \times d \times t}$, where k is the number of keypoints, d is their dimensionality, and t is the number of frames. This matrix is then convolved with a filter θ that has c channels:

$$g_{\theta}(x_t) = \theta * v(x) \quad (2)$$

The spatial dimension of the kernels θ spans the entirety of the key-point dimension, and the temporal dimension spans roughly a second of time. Each kernel outputs a feature f , where $f \in \mathbb{R}^{1 \times t}$. Since there are c channels, the resulting output from the temporal convolution layer is a sequence of t embeddings e_1, \dots, e_t , s.t. $e \in \mathbb{R}^{128}$. Convolutions excel at detecting subtle motion patterns, which makes this a very good embedding for the next part of the architecture. Additionally, convolution is designed for spatial invariance which is why we chose to make the spatial dimension of the kernel match the number of coordinates, otherwise motion

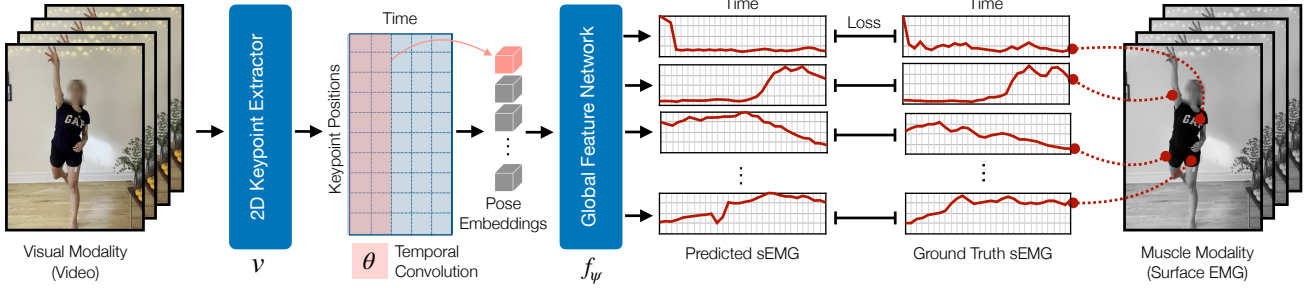


Figure 5. **Our Transformer Architecture.** We illustrate our architecture, composed of the local motion encoder g_θ and the global feature encoder f_ψ . The inputs are frames from a video, and the outputs are the regressed sEMG values for each of the 8 muscles. We supervise on the ground truth sEMG values over time, per muscle.

patterns for legs would need to correspond to similar muscle activation patterns as motion patterns for arms, for example. However, the same motion in pattern in different limbs correspond to drastic differences in muscle activations, as previously explained by comparing gravity’s relationship to hands and feet. The local motion encoder is local temporally, but global spatially.

The second part of our architecture, the global feature network, needs to identify long range patterns in order to capture the dynamics of the muscles in the human body. It is global temporally. We implement it using a Transformer [45] with 4 layers with 8 attention heads and no attention masking. The input to the Transformer is the sequence of coordinate embeddings e_1, \dots, e_t , s.t. $e \in \mathbb{R}^{128}$. The output of the Transformer is another sequence of embeddings o_1, \dots, o_t , s.t. $o \in \mathbb{R}^{128}$. In order to map this sequence to a sequence of dimensionality that corresponds to the number of muscles, we implement a fully connected layer that maps each embedding $o \in \mathbb{R}^{128}$ to an output vector $m \in \mathbb{R}^n$, where n corresponds to the n muscles.

4.4. Learning and Optimization

During learning, we will have pair of video, x , and ground truth sEMG signals, y . Over a training set, the parameters of the neural networks ϕ and θ are optimized in order to minimize the mean squared error objective between the ground truth, y and our prediction \hat{y} :

$$\min_{\psi, \theta} \mathbb{E}_{(x_t, y_t)} [\mathcal{L}(\hat{y}_t, y_t)] \quad (3)$$

We use back-propagation with the Adam [19] optimizer in order to minimize this objective.

4.5. Implementation Details

The length of the input and output sequences is 30, corresponding to 3 seconds with 10 frames per second (fps). The videos were collected on a stand iPhone X with 30 fps, and we downsample the video to 10 frames per second to match the sampling frequency of the EMG sensors at 10 fps. The

convolutional models were trained with batch size 8 on a NVIDIA RTX 2080 Ti GPUs. This computation took approximately 2 hours. Our Transformer models were trained with batch size 32 on a NVIDIA RTX 2080 Ti GPU. This computation took approximately 6 hours. We optimized both with the Adam optimizer [19], using a learning rate of 5×10^{-6} .

5. Experiments

To evaluate our results, we introduce several baselines below, and compare their results across the 20 exercises using root mean squared error as our metric.

5.1. Baselines

Random. The first approach towards solving this problem is to randomly select a sequence of sEMG values from any video in the training set that contains the same exercise as the given video from the test set.

Nearest Neighbor (NN). The second approach towards solving this problem is to perform nearest neighbor on extracted 2D keypoints. To do this, given x_{test} in the test set, we search for a skeleton x_{train} in the training set which has the lowest mean squared error with x_{test} . We then assign x_{train} ’s sEMG values for x_{test} .

Convolutional Model. For our convolutional model baseline, we similarly extract keypoints from our sequence of images x_1, \dots, x_t with VIBE’s pretrained network v , resulting in a matrix M where $M \in \mathbb{R}^{k \times d \times t}$. We flatten M to M' , where $M' \in \mathbb{R}^{kd \times t}$. M' is then processed by 5 separate convolutional layers. Whereas in our Transformer network the dimensionality of each embedding per time bin was the concatenation of the channels (i.e. the number of kernels), here we calculate kernel dimensions to directly reduce the input dimension kd to n across all time bins t . Unlike in our Transformer’s temporal convolution layer, the spatial dimension of the kernels for this baseline are less than kd . As such, these convolutional layers are spatio-temporal. Finally, we include three 2D batch normaliza-

Exercise	Rand.	In-Distribution			Out-of-Distribution		
		NN	CNN	Transf	NN	CNN	Transf
Jumping-Jack	21.3	12.1	9.2	8.8	27.7	23.1	20.9
High-Kick	21.7	13.0	9.8	9.2	18.4	15.1	15.9
Leg-Back	23.0	18.7	10.2	8.8	17.8	14.4	13.6
Front-Kick	12.5	10.1	8.1	7.0	13.2	9.0	10.0
Front-Punch	23.1	14.7	9.8	9.2	19.8	12.7	12.2
Hook-Punch	25.1	12.5	10.6	10.1	17.0	15.3	13.2
Pirouette	20.6	14.0	9.7	10.2	21.5	15.8	15.4
Skater	20.1	10.5	8.1	7.4	20.4	13.5	14.4
Twist	10.5	8.9	5.9	5.4	12.1	11.7	10.3
Squats	15.6	9.6	7.0	7.2	20.2	12.8	11.7
Cross	20.7	13.3	8.2	7.8	19.4	14.4	14.4
Elbow-Punch	19.4	13.3	10.7	10.4	16.1	12.5	11.9
Side-Shuffle	10.4	9.8	7.4	6.8	14.0	13.0	11.1
Batting	25.5	14.5	10.73	10.6	22.5	18.2	19.9
Side-Lunge	24.4	9.5	7.6	6.5	17.7	15.6	14.0
Run	13.8	11.1	8.1	7.8	22.7	16.2	16.9
Ball-Throw	25.6	16.1	11.6	11.4	21.3	15.8	16.3
Bowling	22.5	13.5	11.1	10.8	20.9	15.6	15.7
Knee-Kick	21.4	15.7	11.4	11.2	17.7	18.6	15.7
Woodchop	25.4	13.6	11.0	10.6	23.2	17.0	17.3
Mean	20.7	13.2	9.4	9.0	19.5	15.2	14.7

Table 1. **RMSE per Exercise:** We show performance for both in-distribution and out-of-distribution exercises. The out-of-distribution column shows leave-one-exercise-out, where the model needs to generalize to exercises not seen before by interpolating between the others.

tion [15] layers after the first three convolutional layers, and use ReLu activation functions between each layer. Please refer to the supplemental for further details.

5.2. Results

We report the root mean squared error per exercise, per model, in Table 1. For all but one of the exercises from the 20 exercises, our Transformer model outperforms our random, nearest neighbor retrieval, and convolutional model baselines. The performance stays relatively consistent the 20 exercises. We show two qualitative examples of muscle activation for all 8 muscles from video in Figure 6. The first column is an example of the results for the first subject performing a pirouette, and the second column is an example of results for the second subject throwing a ball. The axis are scaled to the range of values per example per muscle, and we denote the absolute value with a gradient from yellow (low activation) to red (high activation). Even when the range of the sEMG signal is small, indicated by a plot that stays mostly one color, we notice that the predictions follow the ground-truth fairly closely. The alignment of the prediction and ground-truth is often close, illustrating a small error

in phase.

5.3. Generalization

Out-of-Distribution Exercises. We performed a second set of experiments, where we retrained a network on 20 different datasets, each dataset leaving out one exercise. For each model, we then ran inference on the exercise that was left out and reported it in Table 1. The results show that generalization to unseen exercises is possible, and the learning methods always outperform the nearest neighbor method. Further, the Transformer method is on average the best learning-based method. Without seeing every exercise, even with a small dataset, the learning-based benchmarks are able to generalize to new exercises.

Transferring to New Subjects. We also performed experiments to evaluate how well a model trained on one subject can adapt to another. There are three principle reasons for a distribution shift across subjects. First, while the two subjects performed the same set of 20 exercises similarly, the muscle groups that were activated were not always identical. Second, subjects will always vary in body mass, height, and muscle strength. Finally, while we tried to place the sensors identically as possible across the subjects, human error likely caused the sensors locations to deviate. sEMG data is very sensitive to location placement [13]. Nonetheless, the muscle activations across subjects for a given exercise shared similar traits since both subjects muscles’ operate under the same rough rules of the musculoskeletal system. This led us to believe that a model trained on the second subject’s data would benefit from being fine-tuned from a pretrained model on the first subject’s data.

To evaluate this, we fine-tuned the model trained on the first subject with data from the second-subject. We increase the number of exercises included in the dataset. We repeated this for models trained from scratch. We report these results in Figure 7. In both the fine-tuned models and the models trained from scratch, as the number of activities in the second dataset increases, the performance on the second subject’s activities improves, but the fine-tuned models always perform better than those trained from scratch. This result suggests that these representations can be shared across people, with a relatively small dataset for fine-tuning.

Time (s)	0.0	0.5	1.0	1.5	2.0	2.5	3.0
NN	16.6	14.2	13.1	13.0	12.9	13.0	13.3
CNN	13.0	11.2	10.6	10.1	9.8	9.5	9.5
Transformer	12.6	11.0	9.9	9.5	9.2	9.1	9.0

Table 2. **Temporal Analysis.** We compare the RMSE values across our baselines for datasets of varying sequence lengths.

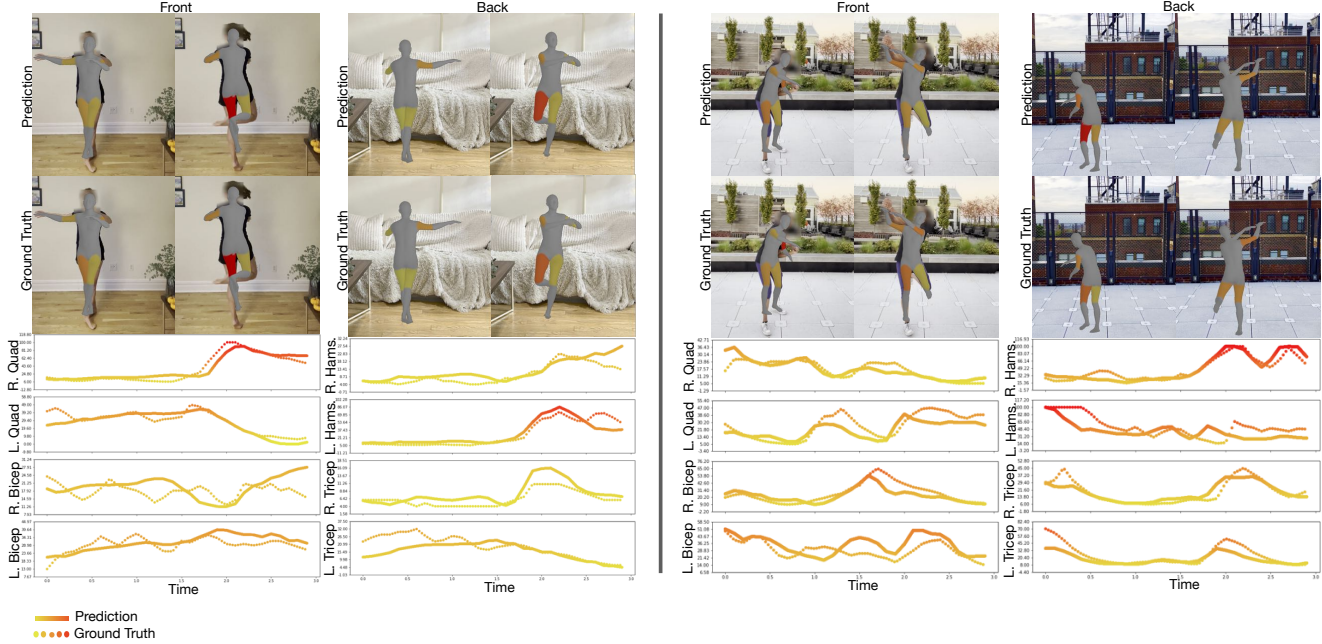


Figure 6. **Qualitative Results.** We illustrate two separate qualitative results. The right example is of the first subject performing a Pirouette. The second example is of the second subject batting. The first row corresponds to a visualization of the predicted activations, and the second row corresponds to a visualization of the ground truth activations. For the plot beneath the frames, the dotted line corresponds to the ground-truth values, and the solid line corresponds to the predictions. Yellow corresponds to relaxed, and red corresponds to flexed.

5.4. Temporal Analysis

In order to evaluate how crucial the temporal component of our model was, we retrained separate Transformer and CNN networks on datasets of 6 different temporal lengths, from ~ 0 to 3 seconds, in increments of 0.5 seconds. ~ 0 seconds here corresponds to a single frame and sEMG value

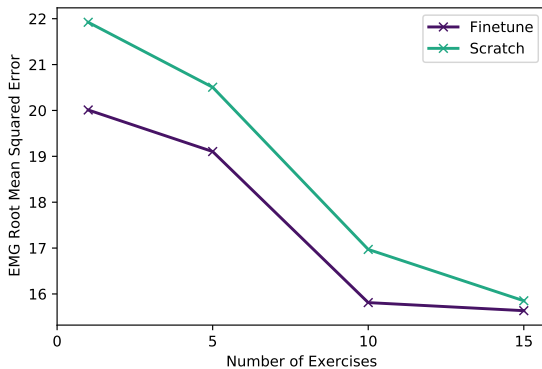


Figure 7. **Transferability to New Subjects.** We illustrate the performance of separate models trained on the second subject’s data with increasing dataset size. The fine-tuned models consistently outperform the models trained from scratch, indicating that the mapping from motion to muscle is transferable across subjects.

per muscle. We also performed nearest neighbor on the same datasets. We notice that for the learning-based methods, the longer the input sequence, the better the performance. The nearest neighbor method however performs worse when the input is longer than 2 seconds.

5.5. Visual Representations from Muscles

Motions that look visually similar do not necessarily correspond to motions that activate similar muscle groups. Intuitively, most people would likely consider jogging and side shuffling to be more similar than jogging and punching. However, the visual modality alone is not sufficient to develop representations of motion that correspond to our intuitive sense of motion similarity, as Euclidian metrics of similarity for human poses do not correspond to musculoskeletal similarity.

To demonstrate this, we create two similarity matrices. Matrix V ’s similarity is computed using only pose data. Matrix MV ’s similarity is computed from our visual representation, which is predictive of muscle activation. Both are shown in Figure 8. Each cell in the matrices correspond to the frequency which the exercise in the column was retrieved, given an instance of an exercise in that row. We used mean squared as our similarity metric for both representations. We ordered the exercises in both matrices such that the matrix V is approximately diagonal. This same diagonal structure does not appear in matrix MV , showing that

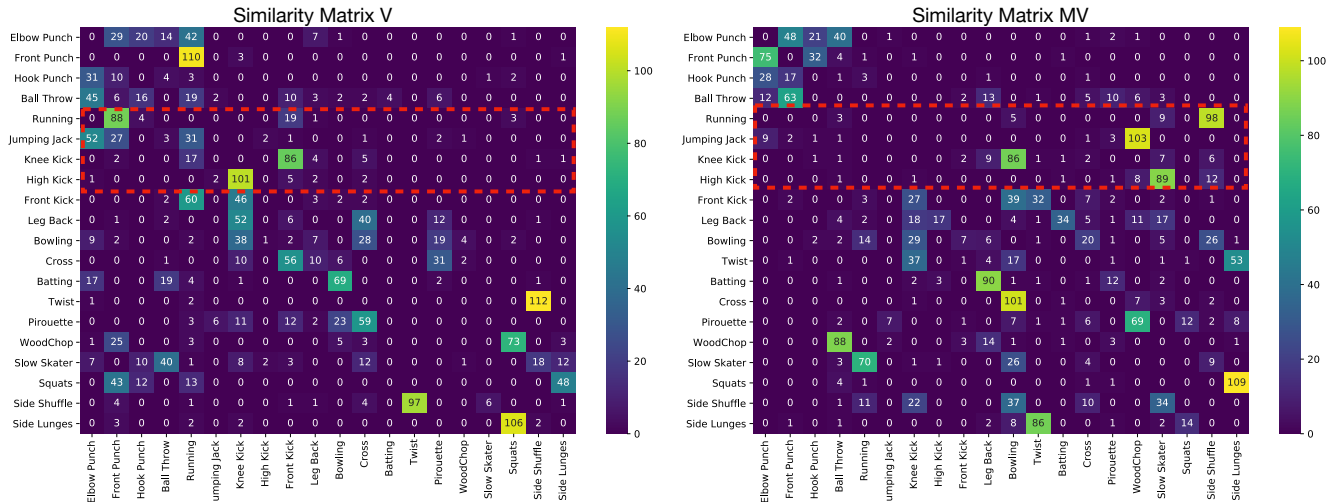


Figure 8. **Similarity Matrices.** We show two similarity matrices. The left matrix corresponds to the retrieval results in the pose space. The right matrix corresponds to the retrieval results for our predicted visual representation, supervised by sEMG. The dashed red boxes serve to highlight that representations that are supervised with muscle data groups activities very differently from standard pose representations.

supervising visual representations from muscle data will group activities very differently from standard visual representations in computer vision.

The distinction between these two representations is illustrated in the cluster in the top half of the matrix, denoted by the red box. This cluster shifts from activating in the left half of the visual similarity matrix to activating in the right half of the muscle similarity matrix. In the visual similarity matrix, the activation in the top left indicates that these exercises are visually similar to each-other and other exercises at the top of the matrix. However, the activation in the top right indicates that these exercises are not muscularly similar to each-other. For instance, running is most similar to front punch in matrix V. This makes sense, since when jogging, our subjects swung their arms back and forth frontally, similar to front punches. However, matrix MV indicates that the most similar exercise would be side shuffle. This also makes sense since side shuffling is effectively the same activity muscularly as running, except moving laterally instead of frontally.

This result highlights how important it is that we integrate muscle activation data in our representations of human motion. The muscle signal teaches the visual perception model to identify motion patterns such that the predicted representations incorporate muscle activation similarity. We share more examples comparing the two similarity matrices in the supplemental material.

6. Conclusion

This paper presents a new visual perception task and dataset for modelling muscle activity from video. We compared several models and showed that Transformers often

outperform other methods at building these representations. Due to the importance of building rich and accurate representations of people, we believe this multimodal signal will be useful for many applications in sports, fitness, and AR/VR.

Acknowledgements: This research is based on work partially supported by the NSF NRI Award #1925157. M.C. is supported by the Amazon CAIT PhD fellowship. The views and conclusions contained herein are those of the authors and should not be interpreted as necessarily representing the official policies, either expressed or implied, of the sponsors.

References

- [1] Kfir Aberman, Mingyi Shi, Jing Liao, Dani Lischinski, Baoquan Chen, and Daniel Cohen-Or. Deep video-based performance cloning. In *Computer Graphics Forum*, volume 38, pages 219–233. Wiley Online Library, 2019. 2
- [2] Leandro Abraham, Facundo Bromberg, and Raymundo Forradellas. Arm muscular effort estimation from images using computer vision and machine learning. In *Ambient Intelligence for Health*, pages 125–137. Springer, 2015. 2
- [3] Yazan Abu Farha, Alexander Richard, and Juergen Gall. When will you do what?-anticipating temporal occurrences of activities. In *Proceedings of the IEEE conference on computer vision and pattern recognition*, pages 5343–5352, 2018. 2
- [4] Pradchaya Anantamek and Narit Hnoohom. Recognition of yoga poses using emg signals from lower limb muscles. In *2019 Joint International Conference on Digital Arts, Media and Technology with ECTI Northern Section Conference on Electrical, Electronics, Computer and Telecommunications*

- Engineering (ECTI DAMT-NCON)*, pages 132–136. IEEE, 2019. 2
- [5] Relja Arandjelovic and Andrew Zisserman. Look, listen and learn. In *Proceedings of the IEEE International Conference on Computer Vision*, pages 609–617, 2017. 2
- [6] Yusuf Aytar, Carl Vondrick, and Antonio Torralba. Soundnet: Learning sound representations from unlabeled video. *Advances in neural information processing systems*, 29, 2016. 2
- [7] Zhe Cao, Tomas Simon, Shih-En Wei, and Yaser Sheikh. Realtime multi-person 2d pose estimation using part affinity fields. In *Proceedings of the IEEE conference on computer vision and pattern recognition*, pages 7291–7299, 2017. 2, 3
- [8] Caroline Chan, Shiry Ginosar, Tinghui Zhou, and Alexei A Efros. Everybody dance now. In *Proceedings of the IEEE/CVF international conference on computer vision*, pages 5933–5942, 2019. 2
- [9] Francesco Di Nardo, Antonio Nocera, Alessandro Cucchiarelli, Sandro Fioretti, and Christian Morbidoni. Machine learning for detection of muscular activity from surface emg signals. *Sensors*, 22(9):3393, 2022. 2
- [10] Dave Epstein, Boyuan Chen, and Carl Vondrick. Oops! predicting unintentional action in video. In *Proceedings of the IEEE/CVF conference on computer vision and pattern recognition*, pages 919–929, 2020. 2
- [11] Chuang Gan, Deng Huang, Peihao Chen, Joshua B Tenenbaum, and Antonio Torralba. Foley music: Learning to generate music from videos. In *European Conference on Computer Vision*, pages 758–775. Springer, 2020. 2
- [12] Ruohan Gao, Tae-Hyun Oh, Kristen Grauman, and Lorenzo Torresani. Listen to look: Action recognition by previewing audio. In *Proceedings of the IEEE/CVF Conference on Computer Vision and Pattern Recognition*, pages 10457–10467, 2020. 2
- [13] Hermie J Hermens, Bart Freriks, Catherine Disselhorst-Klug, and Günter Rau. Development of recommendations for semg sensors and sensor placement procedures. *Journal of electromyography and Kinesiology*, 10(5):361–374, 2000. 6
- [14] Minh Hoai and Fernando De la Torre. Max-margin early event detectors. *International Journal of Computer Vision*, 107(2):191–202, 2014. 2
- [15] Sergey Ioffe and Christian Szegedy. Batch normalization: Accelerating deep network training by reducing internal covariate shift. In *International conference on machine learning*, pages 448–456. PMLR, 2015. 6
- [16] Joseph HR Isaac, Muniyandi Manivannan, and Balaraman Ravindran. Single shot corrective cnn for anatomically correct 3d hand pose estimation. *Frontiers in Artificial Intelligence*, 5, 2022. 2
- [17] Lise A Johnson and Andrew J Fuglevand. Evaluation of probabilistic methods to predict muscle activity: implications for neuroprosthetics. *Journal of neural engineering*, 6(5):055008, 2009. 2
- [18] Will Kay, Joao Carreira, Karen Simonyan, Brian Zhang, Chloe Hillier, Sudheendra Vijayanarasimhan, Fabio Viola, Tim Green, Trevor Back, Paul Natsev, et al. The kinetics human action video dataset. *arXiv preprint arXiv:1705.06950*, 2017. 2
- [19] Diederik P Kingma and Jimmy Ba. Adam: A method for stochastic optimization. *arXiv preprint arXiv:1412.6980*, 2014. 5
- [20] Kris M Kitani, Brian D Ziebart, James Andrew Bagnell, and Martial Hebert. Activity forecasting. In *European conference on computer vision*, pages 201–214. Springer, 2012. 2
- [21] Muhammed Kocabas, Nikos Athanasiou, and Michael J Black. Vibe: Video inference for human body pose and shape estimation. In *Proceedings of the IEEE/CVF conference on computer vision and pattern recognition*, pages 5253–5263, 2020. 2, 3, 4
- [22] Yu Kong, Dmitry Kit, and Yun Fu. A discriminative model with multiple temporal scales for action prediction. In *European conference on computer vision*, pages 596–611. Springer, 2014. 2
- [23] Yu Kong, Zhiqiang Tao, and Yun Fu. Deep sequential context networks for action prediction. In *Proceedings of the IEEE conference on computer vision and pattern recognition*, pages 1473–1481, 2017. 2
- [24] Colin Lea, Michael D Flynn, Rene Vidal, Austin Reiter, and Gregory D Hager. Temporal convolutional networks for action segmentation and detection. In *proceedings of the IEEE Conference on Computer Vision and Pattern Recognition*, pages 156–165, 2017. 2
- [25] Zhan Li, David Guiraud, and Mitsuhiro Hayashibe. Inverse estimation of multiple muscle activations from joint moment with muscle synergy extraction. *IEEE journal of biomedical and health informatics*, 19(1):64–73, 2014. 2
- [26] Lingjie Liu, Weipeng Xu, Michael Zollhoefer, Hyeonwoo Kim, Florian Bernard, Marc Habermann, Wenping Wang, and Christian Theobalt. Neural rendering and reenactment of human actor videos. *ACM Transactions on Graphics (TOG)*, 38(5):1–14, 2019. 2
- [27] Yilin Liu, Shijia Zhang, and Mahanth Gowda. Neuropose: 3d hand pose tracking using emg wearables. In *Proceedings of the Web Conference 2021*, pages 1471–1482, 2021. 2
- [28] Matthew Loper, Naureen Mahmood, Javier Romero, Gerard Pons-Moll, and Michael J Black. Smpl: A skinned multi-person linear model. *ACM transactions on graphics (TOG)*, 34(6):1–16, 2015. 2
- [29] Shuang Ma, Zhaoyang Zeng, Daniel McDuff, and Yale Song. Active contrastive learning of audio-visual video representations. *arXiv preprint arXiv:2009.09805*, 2020. 2
- [30] Yoshihiko Nakamura, Katsu Yamane, Yusuke Fujita, and Ichiro Suzuki. Somatosensory computation for man-machine interface from motion-capture data and musculoskeletal human model. *IEEE Transactions on Robotics*, 21(1):58–66, 2005. 2
- [31] Hui Niu, Takahiro Ito, Damien Desclaux, Ko Ayusawa, Yusuke Yoshiyasu, Ryusuke Sagawa, and Eiichi Yoshida. Estimating muscle activity from the deformation of a sequential 3d point cloud. *Journal of Imaging*, 8(6):168, 2022. 2
- [32] Andrew Owens, Phillip Isola, Josh McDermott, Antonio Torralba, Edward H Adelson, and William T Freeman. Visually

- indicated sounds. In *Proceedings of the IEEE conference on computer vision and pattern recognition*, pages 2405–2413, 2016. 2
- [33] Andrew Owens, Jiajun Wu, Josh H McDermott, William T Freeman, and Antonio Torralba. Ambient sound provides supervision for visual learning. In *European conference on computer vision*, pages 801–816. Springer, 2016. 2
- [34] Hyun Soo Park, Jianbo Shi, et al. Force from motion: decoding physical sensation in a first person video. In *Proceedings of the IEEE Conference on Computer Vision and Pattern Recognition*, pages 3834–3842, 2016. 2
- [35] Leonid Pishchulin, Eldar Insafutdinov, Siyu Tang, Bjoern Andres, Mykhaylo Andriluka, Peter V Gehler, and Bernt Schiele. Deepcut: Joint subset partition and labeling for multi person pose estimation. In *Proceedings of the IEEE conference on computer vision and pattern recognition*, pages 4929–4937, 2016. 2
- [36] Michalis Raptis and Leonid Sigal. Poselet key-framing: A model for human activity recognition. In *Proceedings of the IEEE Conference on Computer Vision and Pattern Recognition*, pages 2650–2657, 2013. 2
- [37] Ali Rohan, Mohammed Rabah, Tarek Hosny, and Sung-Ho Kim. Human pose estimation-based real-time gait analysis using convolutional neural network. *IEEE Access*, 8:191542–191550, 2020. 2
- [38] Michael S Ryoo. Human activity prediction: Early recognition of ongoing activities from streaming videos. In *2011 International Conference on Computer Vision*, pages 1036–1043. IEEE, 2011. 2
- [39] Ryusuke Sagawa, Ko Ayusawa, Yusuke Yoshiyasu, and Akihiko Murai. Predicting muscle activity and joint angle from skin shape. In *Proceedings of the European Conference on Computer Vision (ECCV) Workshops*, pages 0–0, 2018. 2
- [40] Masashi Sekiya, Sho Sakaino, and Tsuji Toshiaki. Linear logistic regression for estimation of lower limb muscle activations. *IEEE Transactions on Neural Systems and Rehabilitation Engineering*, 27(3):523–532, 2019. 2
- [41] Hyungeun Song and Yoichi Hori. Inverse muscle group activity estimation based on neuromusculoskeletal system model. In *TENCON 2015-2015 IEEE Region 10 Conference*, pages 1–5. IEEE, 2015. 2
- [42] Chen Sun, Austin Myers, Carl Vondrick, Kevin Murphy, and Cordelia Schmid. Videobert: A joint model for video and language representation learning. In *Proceedings of the IEEE/CVF International Conference on Computer Vision*, pages 7464–7473, 2019. 2
- [43] Yokhesh K Tamilselvam, Jacky Ganguly, Rajni V Patel, and Mandar Jog. Musculoskeletal model to predict muscle activity during upper limb movement. *IEEE Access*, 9:111472–111485, 2021. 2
- [44] Arash Vahdat, Bo Gao, Mani Ranjbar, and Greg Mori. A discriminative key pose sequence model for recognizing human interactions. In *2011 IEEE International Conference on Computer Vision Workshops (ICCV Workshops)*, pages 1729–1736. IEEE, 2011. 2
- [45] Ashish Vaswani, Noam Shazeer, Niki Parmar, Jakob Uszkoreit, Llion Jones, Aidan N Gomez, Łukasz Kaiser, and Illia Polosukhin. Attention is all you need. *Advances in neural information processing systems*, 30, 2017. 5
- [46] Carl Vondrick, Hamed Pirsiavash, and Antonio Torralba. Anticipating visual representations from unlabeled video. In *Proceedings of the IEEE conference on computer vision and pattern recognition*, pages 98–106, 2016. 2
- [47] Ting-Chun Wang, Ming-Yu Liu, Jun-Yan Zhu, Guilin Liu, Andrew Tao, Jan Kautz, and Bryan Catanzaro. Video-to-video synthesis. *arXiv preprint arXiv:1808.06601*, 2018. 2
- [48] Xionghui Wang, Jian-Fang Hu, Jian-Huang Lai, Jianguo Zhang, and Wei-Shi Zheng. Progressive teacher-student learning for early action prediction. In *Proceedings of the IEEE/CVF Conference on Computer Vision and Pattern Recognition*, pages 3556–3565, 2019. 2
- [49] Hu Xu, Gargi Ghosh, Po-Yao Huang, Dmytro Okhonko, Armen Aghajanyan, Florian Metze, Luke Zettlemoyer, and Christoph Feichtenhofer. Videoclip: Contrastive pre-training for zero-shot video-text understanding. *arXiv preprint arXiv:2109.14084*, 2021. 2
- [50] Katsu Yamane, Akihiko Murai, Sadahiro Takaya, and Yoshihiko Nakamura. Muscle tension database for contact-free estimation of human somatosensory information. In *2009 IEEE International Conference on Robotics and Automation*, pages 633–638. IEEE, 2009. 2
- [51] Ye Yuan, Umar Iqbal, Pavlo Molchanov, Kris Kitani, and Jan Kautz. Glamr: Global occlusion-aware human mesh recovery with dynamic cameras. In *Proceedings of the IEEE/CVF Conference on Computer Vision and Pattern Recognition*, pages 11038–11049, 2022. 2



Figure 2. **The MIA dataset.** We illustrate example exercises from our dataset for each of the 20 exercises.